

## Crack Identification in Metallic Materials

Hideo Saotome, Tatsuya Doi, Seiji Hayano and Yoshifuru Saito

College of Engineering, Hosei University, Kajino, Koganei, Tokyo 184, Japan

**Abstract**—In this paper, we propose a novel formulation for the crack identification problem in metallic materials. In this formulation, cracks are regarded as the equivalent field or potential sources due to the discontinuity of conductivity at the crack positions. This means that crack identification problems are reduced to the inverse problems of searching for equivalent sources. The system equation of the inverse problem, derived by discretizing the integral equation, is successfully solved by the sampled pattern matching method. In consequence, fairly good results are obtained even in the case of plural defect problems.

## I. INTRODUCTION

The crack or defect identification problem in metallic materials is of paramount importance in the safety inspections of aircraft, ships, iron bridges, nuclear reactors and so forth [1]. Identifying crack shape, size and position is the most important objective in nondestructive testing. Therefore, various methods, such as eddy current testing, X-ray computed tomography, ultrasonic imaging and the electric potential method, have been developed. These are in essence reduced to solving the inverse problem.

Numerical methods are widely used as an engineering tool in accordance with the developments of modern digital computers, and applied to solving forward problems in which the electromagnetic field is unknown and solved with its source distribution in space [2]. In most cases, the system equation in the forward problem can be expressed by a regular (non-singular) matrix, which means that the system matrix is square and has its inverse matrix. However, in the inverse problem of which the aim is to obtain the source distribution from the local field information outside the source existing region, the system matrix, obtained by discretizing the governing equation of an integral form, is not usually a regular matrix. Therefore it is difficult to apply the conventional numerical methods used in forward problems to solving the inverse problems.

Metallic structures being examined by nondestructive testings are basically classified into two major categories depending on their shapes. One group consists of flat-shape materials and the other is composed of pillar-shape materials.

In this paper, we propose two kinds of crack identification methods of metallic materials based on electromagnetic field analysis. It is suggested that the magnetic field sensing method is suitable for the defect identification of flat-shape materials and the electric potential sensing method is appropriate to pillar-shape materials, respectively. In both cases, their governing equations can be expressed in an integral form, and they are successfully solved by the sampled pattern matching (SPM) method [3,4].

## II. GOVERNING EQUATIONS

**Magnetic Field Sensing Method**

Most magnetostatic field problems are reduced to solving the following equation assuming the Coulomb gauge  $\nabla \cdot \mathbf{A} = 0$ :

$$(1/\mu) \nabla^2 \mathbf{A} = -\mathbf{J}, \quad (1a)$$

where  $\mu$  is the magnetic permeability,  $\mathbf{A}$  is the magnetic vector potential, and  $\mathbf{J}$  is the current density [5]. Imposing a homogeneous open boundary condition, we have

$$\mathbf{A} = \mu \int G \mathbf{J} dv. \quad (1b)$$

The Green function  $G$  in (1b) for three dimensional fields is given by

$$G = 1/(4\pi r), \quad (2)$$

where  $r$  is a distance between the positions of the current density  $\mathbf{J}$  and of the vector potential  $\mathbf{A}$ . The magnetic field

intensity  $\mathbf{H}$  is obtained from the magnetic flux density  $\mathbf{B}$  as well as the vector potential  $\mathbf{A}$ :

$$\mathbf{H} = (1/\mu) \mathbf{B} = (1/\mu) \nabla \times \mathbf{A}. \quad (3a)$$

Therefore, we have

$$\mathbf{H} = \nabla \times \int G \mathbf{J} dv. \quad (3b)$$

Figure 1 shows a schematic diagram of the magnetic field sensing method. The metallic or conductive material of conductivity  $\sigma$  has a crack in which no current flows. We assume that (3b) is established with the no-crack condition in the material where the current density  $\mathbf{J}$  is uniformly distributed parallel to the  $x$ -axis. On the other hand, if cracks exist in the material, we have

$$\mathbf{H}_d = \nabla \times \int G (\mathbf{J} + \mathbf{J}_s) dv, \quad (4)$$

where  $\mathbf{J}_s$  and  $\mathbf{H}_d$  are the equivalent spring current density caused by the cracks and the magnetic field intensity perturbed by  $\mathbf{J}_s$ , respectively. The current density in a crack is zero, so that the discontinuity of conductivity causes the current density  $\mathbf{J}_s (= -\mathbf{J})$  in the crack. The current density  $\mathbf{J}_s$  faces in the counter direction of the original current density  $\mathbf{J}$ . This means, if the current density  $\mathbf{J}_s$  is toward the counter direction to the current density  $\mathbf{J}$ , then the current density in the crack is zero even though the conductivity  $\sigma$  exists in it. Moreover, the current density  $\mathbf{J}_s$  outside the crack is assumed to diverge from the surface of the crack. As a result, the effect of cracks in the metallic material can be analyzed using  $\mathbf{J} + \mathbf{J}_s$  of (4) without the difficulty of a medium discontinuity problem.

The crack identification of the metallic material is magnetically carried out by measuring the magnetic field intensity  $\mathbf{H}_d$  and solving the following integral equation:

$$\mathbf{H}_d = \mathbf{H} - \mathbf{H} = \nabla \times \int G \mathbf{J}_s dv, \quad (5)$$

where  $\mathbf{H}$  has been obtained from (3b) in advance.

As shown in Fig. 1, discretizing the metallic material into small subdivisions  $\Delta V_j$  ( $j=1, \dots, n$ ), (5) takes the following form:

$$\mathbf{H}_{dz} = \sum_{j=1}^n \frac{\mathbf{J}_{sz} \times \mathbf{a}_{ij} \Delta V_j}{4\pi r_{ij}^2}, \quad i=1, \dots, n. \quad (6)$$

where  $n$  is the number of magnetic field measurement points,  $r_{ij}$  is a distance between the points of  $\mathbf{H}_{dz}$  and  $\mathbf{J}_{sz}$ , and  $\mathbf{a}_{ij}$  is the unit space vector in the direction of  $r_{ij}$ . Equation (6) has been derived by assuming that  $\mathbf{J}_{sz}$  takes a constant value in the small volume  $\Delta V_j$ , viz.,

$$\nabla \times \left( \frac{\mathbf{J}_{sz}}{4\pi r} \right) = \mathbf{J}_{sz} \times \frac{\mathbf{a}_{ij}}{4\pi r_{ij}^2}. \quad (7)$$

Assuming a current dipole vector  $\mathbf{Q}_{sj}$  [Am] defined as

$$\mathbf{Q}_{sj} = \mathbf{J}_{sz} \Delta V_j, \quad (8)$$

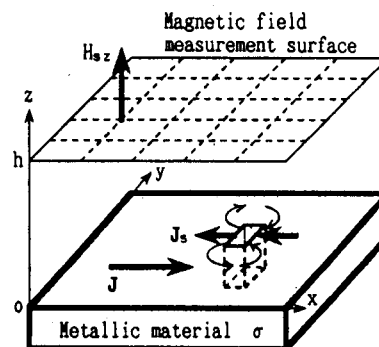


Fig. 1. Model for magnetic field sensing method.

(6) can be rewritten as

$$H_{s_i} = \sum_{j=1}^n |Q_{s_j}| \frac{\mathbf{e}_j \times \mathbf{a}_{j_j}}{4 \pi r_{ij}^2}, \quad i=1, \dots, n, \quad (9)$$

where  $\mathbf{e}_j$  is unit space vector in the direction of  $\mathbf{J}_{s_j}$ . Equation (9) essentially corresponds to the Biot-Savart law and the current dipole is equivalent to the current element which is the product of current and its path length.

### Electric Potential Sensing Method

In a stationary current flowing field as shown in Fig. 2, the relation between the electric potential  $\phi$  and the current density  $\mathbf{J}$  in a metallic material having the conductivity  $\sigma$  is given by [5]

$$-\sigma \nabla \phi = \mathbf{J}. \quad (10)$$

If the metallic material has cracks, (10) can be modified into

$$-\sigma \nabla \phi_d = \mathbf{J} + \mathbf{J}_s, \quad (11)$$

where  $\phi_d$  is the electric potential which has been perturbed by the equivalent current density  $\mathbf{J}_s$  due to the medium discontinuity cause by the cracks. Subtracting (10) from (11) yields

$$\sigma \nabla \phi_s = -\mathbf{J}_s, \quad (12a)$$

where

$$\phi_s = \phi_d - \phi. \quad (12b)$$

The divergence of (12a) becomes

$$\nabla^2 \phi_s = -\nabla \cdot \mathbf{J}_s / \sigma. \quad (13)$$

Equation (13) suggests that the electric potential perturbation  $\phi_s$  caused by cracks can be expressed by the divergence of the equivalent current density  $\mathbf{J}_s$  springing out of the one side and absorbed on the other side of the cracks. When the electric potential  $\phi_s$  has been measured inside the material, the current density  $\mathbf{J}_s$  is easily obtained by substituting it into (12a) or (13). However, in nondestructive testing, the electric potential cannot be measured inside the material, which means only the local electric potential is measurable. Therefore, it is difficult to get a unique solution of  $\mathbf{J}_s$  by solving the differential equation (12a) or (13).

In (13), the left hand side term does not contain the medium parameter  $\sigma$ , so that the electric potential  $\phi_s$  is written in an integral form:

$$\phi_s = \int G (\nabla \cdot \mathbf{J}_s / \sigma) dv, \quad (14)$$

where the Green function  $G$  denotes the geometric relation between the positions of the potential  $\phi_s$  and of its source  $\nabla \cdot \mathbf{J}_s$ . Consequently, the inverse problem of crack identification can be analyzed by solving the integral equation (14).

Discretizing (14) and applying Gauss's theorem to each of subdivisions  $\Delta V_j$  ( $j=1, \dots, m$ ) in the metallic material, we have

$$\begin{aligned} \int_{\Delta U_j} G_{ij} (\nabla \cdot \mathbf{J}_{s_j} / \sigma) dv &= \int_{\Delta S_j} G_{ij} (\mathbf{J}_{s_j} / \sigma) dS \\ &= |\mathbf{I}_{s_j} / \sigma| (G_{ij}^+ - G_{ij}^-) \\ &= |\mathbf{P}_{s_j}| (G_{ij}^+ - G_{ij}^-), \quad i=1, \dots, n, \end{aligned} \quad (15)$$

where  $\Delta S_j$  denotes a surface area of  $\Delta V_j$ ,  $\mathbf{I}_{s_j}$  is a current due to the current density  $\mathbf{J}_{s_j}$ ,  $\mathbf{P}_{s_j}$  is a voltage dipole vector ( $\mathbf{I}_{s_j} / \sigma$ ) [Vm], and  $n$  is a number of measurement points for  $\phi_s$ . The superscripts + and - of the Green function  $G_{ij}$  refer to the positions of the end and starting points of the voltage dipole vector  $\mathbf{P}_{s_j}$ , respectively. The physical meaning of the voltage dipole vector  $\mathbf{P}_{s_j}$  can be interpreted by considering the time derivatives of electric charges  $+q_{s_j}$  and  $-q_{s_j}$  located at a distance  $\delta$  apart as shown in Fig. 3, because the relation between  $\mathbf{P}_{s_j}$  and  $\partial q_{s_j} / \partial t$  can be expressed by

$$\partial q_{s_j} / \partial t = \int_{\Delta U_j} \nabla \cdot \mathbf{J}_{s_j} dv = |\mathbf{I}_{s_j}| = \sigma |\mathbf{P}_{s_j}|. \quad (16)$$

With (15), (14) can be written in the following form:

$$\phi_{s_i} = \sum_{j=1}^n |\mathbf{P}_{s_j}| (G_{ij}^+ - G_{ij}^-), \quad i=1, \dots, n. \quad (17)$$

Consider a circular metallic pillar in which we impressed the current in parallel to the  $z$ -axis as shown in Fig. 2. Under the no-crack condition, the electric potential along the circular contour of the surface at a fixed  $z$ -axis coordinate

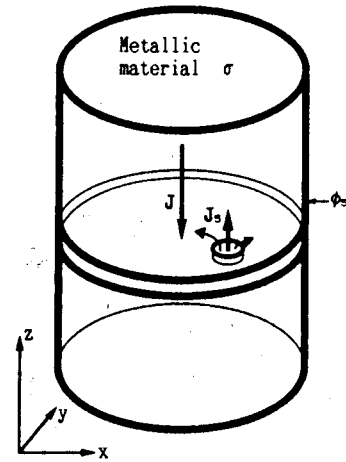


Fig. 2. Model for electric potential sensing method.

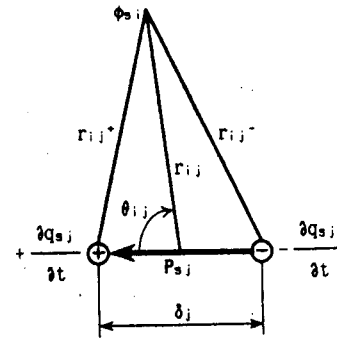


Fig. 3. Electric potential due to the voltage dipole.

takes a constant value. Therefore,  $\phi_s=0$ . However, when a crack exists, the impressed current does not flow through the crack. This disturbed current flow is composed of  $\mathbf{J}+\mathbf{J}_s$ . The  $x$  and  $y$  components of the current density  $\mathbf{J}_s$  cause the electric potential perturbation  $\phi_s$  along the contour of the circular cross section as shown in Fig. 2. Thus, the crack identification can be carried out by searching for the  $x$ - $y$  components of the current density  $\mathbf{J}_s$  or the voltage dipole  $\mathbf{P}_s$  on the cross-sectional  $x$ - $y$  plane from the electric potential distribution measured along the circular contour enclosing the  $x$ - $y$  plane.

In two dimensional fields, the Green function  $G$  is given by

$$G = -\ln r / (2 \pi). \quad (18)$$

Therefore, (17) can be modified into the following form:

$$\phi_{s_i} = \sum_{j=1}^n \frac{|\mathbf{P}_{s_j}|}{2 \pi} (\ln r_{ij}^- - \ln r_{ij}^+), \quad i=1, \dots, n. \quad (19)$$

where  $r_{ij}^+$  and  $r_{ij}^-$  are depicted in Fig. 3. Denoting  $r_{ij}$  as a distance from the middle of the voltage dipole  $\mathbf{P}_s$  to the position of  $\phi_{s_i}$  as shown in Fig. 3 and assuming  $\delta \ll r_{ij}$ , we have

$$r_{ij}^+ \approx r_{ij} (1 - \delta_j \cos \theta_{ij} / (2 r_{ij})), \quad (20a)$$

$$r_{ij}^- \approx r_{ij} (1 + \delta_j \cos \theta_{ij} / (2 r_{ij})), \quad (20b)$$

where  $\theta_{ij}$  is the angle of  $r_{ij}$  referred to the vector  $\mathbf{P}_{s_j}$ . Substituting (20a) and (20b) into (19) yields

$$\begin{aligned} \phi_{s_i} &= \sum_{j=1}^n \frac{|\mathbf{P}_{s_j}|}{2 \pi} \left( \frac{\delta_j}{r_{ij}} \cos \theta_{ij} + \frac{\delta_j^3}{3 r_{ij}^3} \cos^3 \theta_{ij} + \dots \right) \\ &\approx \sum_{j=1}^n |\mathbf{P}_{s_j}| \frac{\delta_j}{2 \pi r_{ij}} \cos \theta_{ij}, \quad i=1, \dots, n, \end{aligned} \quad (21)$$

because  $(\delta_j \cos \theta_{ij} / (2 r_{ij})) < 1$ .

### III. SAMPLED PATTERN MATCHING METHOD

#### System Equation of Inverse Problems

From (5) and (14), it is revealed that the crack identification problem can be reduced to the source position

searching problem of the equivalent spring current density  $J_s$  from local field or potential distribution obtained by measurements. Discretization of (5) and (14) leads to (9) and (21), respectively. Equations (9) and (21) are the system equations of the inverse problems of searching for the crack positions and can be expressed by

$$U = \sum_{j=1}^n \alpha_j d_j, \quad (22)$$

where the vectors  $U$  and  $d_j$  are  $n$ -th order column vectors. In the magnetic field case,  $U$ ,  $d_j$  and  $\alpha_j$  are given by

$$U = [H_{s1}, H_{s2}, \dots, H_{sn}]^T, \quad (23a)$$

$$d_j = \{1/(4\pi)\} [\theta_j \times a_{1j}/r_{1j}^2, \theta_j \times a_{2j}/r_{2j}^2, \dots, \theta_j \times a_{nj}/r_{nj}^2]^T, \quad (23b)$$

$$\alpha_j = |Q_{sj}|. \quad (23c)$$

In the current flowing field case, they are given by

$$U = [\phi_{s1}, \phi_{s2}, \dots, \phi_{sn}]^T, \quad (24a)$$

$$d_j = \{1/(2\pi)\} [(\delta_j/r_{1j})\cos\theta_{1j}, (\delta_j/r_{2j})\cos\theta_{2j}, \dots, (\delta_j/r_{nj})\cos\theta_{nj}]^T, \quad (24b)$$

$$\alpha_j = |P_{sj}|. \quad (24c)$$

**Algorithm for Obtaining a Unique Solution Pattern**

Generally, the number of field or potential source points,  $m$ , is much larger than the number of field or potential measurement points,  $n$ , because measurements are done locally in nondestructive testing. Therefore, the following condition is established in the system equation (22):

$$n \ll m. \quad (25)$$

Because of the condition (25), it is obviously difficult to obtain a unique solution to (22). Namely, the number of equations,  $n$ , is much less than the number of unknowns,  $m$ . In order to surmount this difficulty, we have previously proposed the sampled pattern matching (SPM) method [3,4] to obtain the unique source distribution pattern from (22).

In the SPM method,  $d_j$  in (23b) or (24b) is regarded as a field or potential pattern vector and the source position searching is carried out by means of the Cauchy-Schwarz relation, viz.,

$$\gamma_j = U^T \cdot d_j / (\|U\| \|d_j\|), \quad j=1, \dots, m, \quad (26a)$$

where a norm  $\|\cdot\|$  denotes a summation of root-mean-square values of vector elements. Obviously, the maximum of  $\gamma_j$  identifies the most dominant source position because (26a) reveals the angle or pattern matching rate between the measured pattern vector  $U$  and the field or potential pattern vector  $d_j$  due to the source located at the point  $j$ . Moreover, this calculation takes into account the spatial source vector angle, because the field or potential pattern vector  $d_j$  in (23b) or (24b) depends on not only the current or voltage dipole positions but also their directions in space. After finding the first source point  $k$ , which is called a pilot point and has taken the maximum value of  $\gamma_j$  ( $j=1, \dots, m$ ) in (26a), the second source point can be found by searching for the maximum of

$$\gamma_{kj} = U^T \cdot (d_k + d_j) / (\|U\| \|d_k + d_j\|), \quad j \neq k, \quad j=1, \dots, m. \quad (26b)$$

By continuing with similar procedures to (26a) or (26b), it is possible to obtain the field or potential source distribution pattern:

$$\alpha_1 \frac{\|d_1\|}{\|U\|} \approx \frac{1}{m} \frac{U^T}{\|U\|} \cdot \left( \frac{d_1}{\|d_1\|} + \frac{d_k + d_1}{\|d_k + d_1\|} + \dots \right), \quad (27a)$$

$$\alpha_2 \frac{\|d_2\|}{\|U\|} \approx \frac{1}{m} \frac{U^T}{\|U\|} \cdot \left( \frac{d_2}{\|d_2\|} + \frac{d_k + d_2}{\|d_k + d_2\|} + \dots \right), \quad (27b)$$

$$\alpha_k \frac{\|d_k\|}{\|U\|} \approx \frac{1}{m} \left( \frac{U^T}{\|U\|} \cdot \frac{d_k}{\|d_k\|} + 1 + 1 + 1 + \dots \right), \quad (27c)$$

$$\alpha_n \frac{\|d_n\|}{\|U\|} \approx \frac{1}{m} \frac{U^T}{\|U\|} \cdot \left( \frac{d_n}{\|d_n\|} + \frac{d_k + d_n}{\|d_k + d_n\|} + \dots \right), \quad (27d)$$

where  $m$  denotes the number of the found pilot points. Equations (27a)-(27d) give a unique solution pattern, not the exact solutions [3,4].

**V. EXAMPLES**

**Magnetic Field Sensing Method**

In order to verify the validity of the magnetic field sensing method, test examples with one and plural cracks are demonstrated.

The magnetic field intensity  $H_{sz}$  normal to the measurement surface shown in Fig. 1 is used for the crack identification. The height  $h$  of the measurement surface is 0.104 normalized by the length of the square material side. Figures 4(a) and 4(b) show the results of crack identification by means of (22) with (23a), (23b) and (23c). A crack located at  $(x_1, y_1)$  in Fig. 4(a) and two cracks located at  $(x_1, y_1)$  and  $(x_2, y_2)$  in Fig. 4(b) are assumed to have the same square size,  $0.042 \times 0.042$ , normalized by the material size. The current distributions perturbed by the cracks have been computed by the FEM and the magnetic field perturbations  $H_{sz}$  for these test examples have been obtained from the computed current distributions.

In the problem of Fig. 4(a), the number of measurement points is  $2 \times 2 = 4$  located at the vertices of the measurement surface shown in Fig. 1. The small solid circle with a needle shows the most dominant current dipole vector obtained from (27a)-(27d). The needle refers to the spatial direction of the current dipole, in this case, the current dipole is leftward because the impressed current flows in the positive  $x$  direction as shown in Fig. 1. The current dipole equivalent to the crack located at  $(x_1, y_1)$  is successfully obtained by the SPM method.

In order to obtain the result of Fig. 4(b), regularly spaced  $6 \times 6 = 36$  magnetic field measurement points on the surface in Fig. 1 were used. The vectors shown in Fig. 4(b) are the top 20% results of (27a)-(27d) obtained by taking account of the spatial angles of the current dipoles.

In a plural crack case, the equivalent currents of the cracks are disturbed by their mutual interference. This makes the problem more difficult. In order to overcome this difficulty, the improved SPM method has been applied to the problem of Figs. 5(a) and 5(b), where the metallic materials have plural cracks depicted by squares with a slanted line. The current dipoles equivalent to the cracks are directed toward

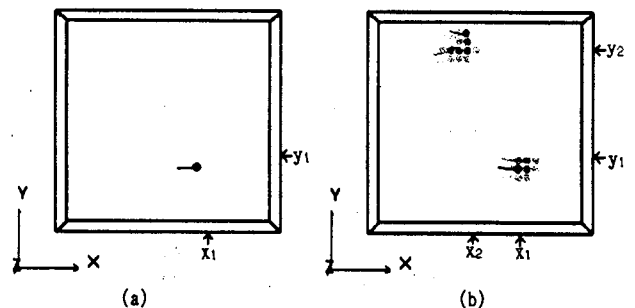


Fig. 4. Crack position identification by measuring magnetic field intensity. Representation by the current dipoles. (a)One crack. (b)Two cracks.

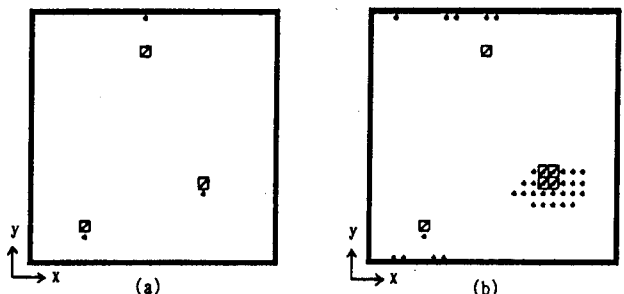


Fig. 5. Crack position identification by measuring magnetic field intensity. Representation by the pilot points. (a)Three cracks. (b)One large and two small cracks.

the counter direction of the impressed current. Therefore, we should search for the current dipoles satisfying this condition, i.e. the negative  $x$  direction. This method is carried out by searching for the pilot points where the  $x$  component of the current dipole takes the maximum of  $\gamma_j$  in (26a),  $\gamma_{kj}$  in (26b), and so forth. In Figs. 5(a) and 5(b), the found pilot points are depicted by the dots. The results in those figures were obtained from the magnetic field measured at  $n=6 \times 6=36$  regularly spaced points at the same height as in Fig. 4. In Fig. 5(a), the SPM process has been continued until  $\gamma$  reaches its peak value. As a result, the number of the found pilot points,  $m'$ , is three. From the result in Fig. 5(a), it is revealed that the found pilot points have been located near the cracks. In Fig. 5(b), the SPM process has been continued until the number of pilot points,  $m'$ , reaches the number of measurement points, i.e.  $m'=n=36$ . Figure 5(b) shows that a large crack can be identified by the concentration rate of the found pilot points.

#### Electric Potential Sensing Method

To demonstrate the electric potential sensing method, we will pose test problems.

Figures 6(a) and 6(b) show the results obtained by the electric potential sensing method. The triangles in those figures refer to the cracks on the circular  $x$ - $y$  plane as shown in Fig. 2. The current density  $J_s$  on the surface just above the crack shown in Fig. 2 is mainly directed to the center of the circular cross section of the pillar. Therefore, the SPM procedure is carried out on the  $x$ - $y$  plane by searching for only the voltage dipoles in the radial direction toward the middle of the pillar. The dots in Fig. 6(a) and 6(b) show the found pilot points. In Fig. 6(a), the number of the pilot points is  $m'=5$  which has been obtained up to the first peak of  $\gamma$ , and the number of measurement points is  $n=72$ . Also, in Fig. 6(b), the SPM process was continued up to the  $m'=n=72$  points. From Figs. 6(a) and 6(b), it is revealed that the crack positions and sizes can be identified from the electric potential perturbation measured along the contour of the metallic material.

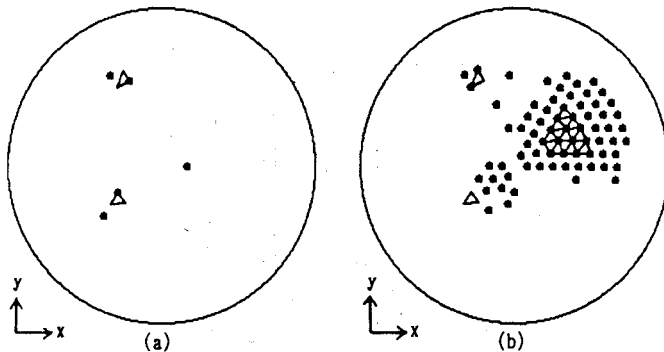


Fig. 6 Crack position identification by measuring electric potential. Representation by the pilot points. (a) Two cracks. (b) One large and two small cracks.

#### V. CONCLUSION

As shown above, we have proposed a promising method for the nondestructive testing of metallic materials. Also, it has been revealed that the magnetic field and electric potential sensing methods are suitable for the crack identification of

the flat- and pillar-shape materials, respectively. The novel formulation, based on the equivalent field or potential source corresponding to the discontinuity of conductivity, has been proposed for the crack identification problems. As a result, it has been demonstrated that a combination of the SPM method with our new formulation is capable of estimating the positions and sizes of the cracks even though the material has plural cracks.

#### REFERENCES

- [1] S. R. H. Hoole, et al., "Inverse problem methodology and finite elements in the identification of cracks, sources, materials, and their geometry in inaccessible locations," *IEEE Trans. Magn.*, vol. 27, pp. 3433-3443, May 1991.
- [2] Y. Saito, et al., "Finite element solution of unbounded magnetic field problem containing ferromagnetic materials," *IEEE Trans. Magn.*, vol. MAG-24, No. 6, pp. 2946-2948, Nov. 1988.
- [3] Y. Saito, et al., "A formulation of the inverse problems in magnetostatic fields and its application to a source position searching of the human eye fields," *J. Appl. Phys.*, vol. 67, No. 9, May 1990, pp. 5830-5832.
- [4] H. Saotome, et al., "Inverse problem in biomagnetic fields," *Trans. IEE, Japan*, vol. 112-A, No. 4, April 1992, pp. 279-286.
- [5] S. R. H. Hoole, "Computer Aided Analysis and Design of Electromagnetic Devices," New York: Elsevier, 1989.

Hideo Saotome was born in Tokyo, Japan, on December 13, 1958. He received the B.E. and M.E. degrees in electrical engineering from Hosei University, Tokyo in 1981 and 1983, respectively. In 1981, he was a visiting postgraduate student at McGill University, Montreal.

Since 1983, he has worked for Fuji Electric Co., Ltd. in the power electronics department. He is currently studying for a doctorate on inverse problems at Hosei University.

Tatsuya Doi was born in Kanagawa, Japan, on May 9, 1969. He received the B.E. degree in electrical engineering at Hosei University, Tokyo in 1992.

He is currently a master's course student of the Graduate School at Hosei University and his present interest is nondestructive testing.

Seiji Hayano was born in Tokyo, Japan, on July 6, 1947. He received the B.E. degree in electrical communication engineering from Tokai University, Tokyo in 1972 and the M.E. degree in electrical engineering from Hosei University, Tokyo in 1977.

He is currently an instructor in the Department of Electrical Engineering at Hosei University. His main interest is magnetic field analysis.

Yoshifuru Saito was born in Fukuoka, Japan, on July 24, 1946. He received the B.E., M.E. and Ph.D degrees in electrical engineering from Hosei University, Tokyo in 1969, 1971 and 1975, respectively. In 1981, Dr. Saito was a visiting researcher at McGill University, Montreal.

He is currently a Professor in the Department of Electrical Engineering at Hosei University. His present interests are electromagnetodynamics including the modelings of magnetic materials, semiconductor simulator, computational electro-dynamics, spurious problem in eigen value, inverse problems and biomagnetics.